

Adaptive ADMM in Distributed Radio Interferometric Calibration

Sarod Yatawatta*

ASTRON,

The Netherlands Institute for Radio Astronomy,
Dwingeloo, The Netherlands
Email: yatawatta@astron.nl*

Faruk Diblen and Hanno Spreew

Netherlands eScience Center

Science Park 140 (Matrix I)

1098 XG Amsterdam, The Netherlands

Abstract—Distributed radio interferometric calibration based on consensus optimization has been shown to improve the estimation of systematic errors in radio astronomical observations. The intrinsic continuity of systematic errors across frequency is used by a consensus polynomial to penalize traditional calibration. Consensus is achieved via the use of alternating direction method of multipliers (ADMM) algorithm. In this paper, we extend the existing distributed calibration algorithms to use ADMM with an adaptive penalty parameter update. Compared to a fixed penalty, its adaptive update has been shown to perform better in diverse applications of ADMM. In this paper, we compare two such popular penalty parameter update schemes: residual balance penalty update and spectral penalty update (Barzilai-Borwein). We apply both schemes to distributed radio interferometric calibration and compare their performance against ADMM with a fixed penalty parameter. Simulations show that both methods of adaptive penalty update improve the convergence of ADMM but the spectral penalty parameter update shows more stability.

Keywords—Distributed calibration, Interferometry: Radio interferometry

I. INTRODUCTION

Raw data produced by radio interferometric arrays are almost always corrupted by systematic errors introduced by the propagation medium (atmosphere) and by the instrument (beam and receiver). Calibration is estimation of such errors and correcting the data to remove the effects of such errors. In order to handle large volumes of data produced by modern radio interferometric arrays, efficient and accurate calibration algorithms are necessary. The recent surge in popularity of distributed optimization algorithms [1], [2] have enabled us to address some of these issues related to calibration of large data volumes in radio astronomy.

With the use of consensus optimization [2], it has been shown that [3], [4] distributed calibration provides a way of distributing the computational burden over a network of computers while at the same time improving the quality of calibration. This enables processing of huge amounts of data that are already stored at various locations across a network of computers and using the local computational power available at each particular location with minimal network communication. In order to do this, the inherent continuity of systematic errors over frequency is exploited and this is added as a constraint onto calibration. With this modification, calibration is transformed into a consensus optimization [2] problem and we use alternating direction method of multipliers (ADMM)

[1] as the underlying algorithm to reach consensus. Similar distributed computing strategies are being developed in radio interferometric imaging as well [5]–[8].

There is widespread use of the ADMM algorithm in various and diverse applications including machine learning [2], [9], image processing [10] and medical imaging [11]. Unlike most applications, radio interferometric calibration using ADMM has some unique properties. The cost function that is minimized in calibration is nonlinear and nonconvex. Even though the systematic errors (e.g., ionosphere, beam shape, receiver gain) have well behaved continuity, the exact description of this behavior using polynomials of low degree is not accurate enough. This is due to the complex interactions of the systematic errors, especially when a wide area of the sky is observed. Therefore, consensus can be achieved only based on an approximate model, which is clearly different than most other application. Furthermore, while most other applications use complicated network topologies, we use a simpler topology with a set of data processing nodes connected to one fusion center.

The convergence rate of ADMM and its dependence on the penalty parameter are well studied and generally with proper initialization [12]–[16] and also with adaptive update [2], [17]–[21], it has been shown that convergence could be improved. Our previous work [22] focused on the initialization of the penalty parameter using the smallest eigenvalue of the Hessian of the cost function. In this paper, we further improve our calibration by enabling adaptive update of the penalty parameter. We compare two adaptive penalty parameter update schemes in this paper. The first scheme is *residual balancing* [2], [17], [18] where the penalty is updated to balance the primal and dual residuals of the ADMM algorithm. In contrast, the second method is based on the *spectral* penalty parameter update [19]–[21], which is based on the Barzilai-Borwein adaptive step size selection method [23] in gradient descent. We compare both methods using simulated radio interferometric data and both methods give better performance than the case where the penalty parameter is kept fixed. Radio astronomical observations (even made by the same interferometric array) have varying instrumental models depending on the direction of the sky being observed and the frequency range and time interval at which data is taken. Therefore, we find that the residual balancing method needs proper tuning [18] to suit each particular observation. On the other hand, the spectral penalty update is less prone to changes in instrumental

model and is better suited in processing large data volumes with minimal manual intervention.

The rest of the paper is organized as follows: In section II we give an overview of distributed radio interferometric calibration using consensus optimization. In section III, we present schemes for updating the penalty parameter with ADMM iterations. Simulation results are presented in section IV where we demonstrate the improved performance with an adaptive penalty parameter. Finally, we draw our conclusions in section V.

Notation: Matrices and vectors are denoted by bold upper and lower case letters as \mathbf{J} and \mathbf{v} , respectively. The transpose and the Hermitian transpose are given by $(\cdot)^T$ and $(\cdot)^H$. The matrix Frobenius norm is given by $\|\cdot\|$. The set of real and complex numbers are denoted by \mathbb{R} and \mathbb{C} respectively. The identity matrix is given by \mathbf{I} . The matrix trace operator is given by $\text{trace}(\cdot)$.

II. RADIO INTERFEROMETRIC CALIBRATION

We consider an interferometric array consisting of N stations. The radiation originating from any given direction in the sky is seen at the interferometer formed by stations p and q as \mathbf{V}_{pqf} [24]

$$\mathbf{V}_{pqf} = \mathbf{J}_{pf}\mathbf{C}_{pqf}\mathbf{J}_{qf}^H + \mathbf{N}_{pqf} \quad (1)$$

where f is the frequency at which data is taken and $\mathbf{V}_{pqf}, \mathbf{J}_{pf}, \mathbf{J}_{qf}, \mathbf{C}_{pqf}, \mathbf{N}_{pqf} \in \mathbb{C}^{2 \times 2}$. The error-free signal from the sky is given by \mathbf{C}_{pqf} , which is essentially the Fourier transform of the sky model and can be pre-computed [25]. The systematic errors corrupting the true signal are given by the Jones matrices $\mathbf{J}_{pf}, \mathbf{J}_{qf}$. The noise is given by \mathbf{N}_{pqf} and is assumed to have complex, zero mean, circular Gaussian elements.

In reality, the observed data is the sum of many signals as in (1), originating from many directions in the sky. However, we can simplify calibration along many such directions in the sky using the space alternating generalized expectation maximization (SAGE) algorithm [26], [27]. In this paper, we describe our algorithms for calibration along a single direction but the results presented in section IV is based on calibration along multiple directions.

The cost function that is minimized is given as

$$g_f(\mathbf{J}_f) = \sum_{p,q} \|\mathbf{V}_{pqf} - \mathbf{A}_p \mathbf{J}_f \mathbf{C}_{pqf} (\mathbf{A}_q \mathbf{J}_f)^H\|^2 \quad (2)$$

where the systematic errors for all N stations are grouped as $\mathbf{J}_f \in \mathbb{C}^{2N \times 2}$,

$$\mathbf{J}_f \triangleq [\mathbf{J}_{1f}^T, \mathbf{J}_{2f}^T, \dots, \mathbf{J}_{Nf}^T]^T. \quad (3)$$

Using the canonical selection matrix $\mathbf{A}_p \in \mathbb{R}^{2 \times 2N}$, where only the p -th block is $\mathbf{I} \in \mathbb{R}^{2 \times 2}$,

$$\mathbf{A}_p \triangleq [\mathbf{0}, \mathbf{0}, \dots, \mathbf{I}, \dots, \mathbf{0}], \quad (4)$$

we can select the systematic errors for the station p as $\mathbf{A}_p \mathbf{J}_f$. Note that in (2), the summation is taken over all the baselines pq that have data, within a small bandwidth and time interval within which the systematic errors are assumed to be fixed.

The variation of \mathbf{C}_{pqf} in (2) with f is smooth and is known. Moreover, the variation of the systematic errors \mathbf{J}_f is assumed smooth, but not exactly known. While conventional calibration minimizes (2) without exploiting this smoothness, we can add this as an additional constraint. Given that data is collected at a set of frequencies $\mathcal{F} = \{f_1, f_2, \dots, f_P\}$, the reformulated calibration problem can be stated as [3]

$$\mathbf{J}_f = \arg \min_{\mathbf{J}} g_f(\mathbf{J}) \text{ subject to } \mathbf{J}_f = \mathbf{B}_f \mathbf{Z}, \forall f \in \mathcal{F}. \quad (5)$$

In (5), the constraint $\mathbf{J}_f = \mathbf{B}_f \mathbf{Z}$ enforces the continuity of \mathbf{J}_f with f . In order to do this, we use $\mathbf{B}_f \in \mathbb{R}^{2N \times 2NF}$ which is a set of F basis functions in frequency (we use the same basis functions for all N stations) and $\mathbf{Z} \in \mathbb{C}^{2NF \times 2}$ is the global variable that enforces continuity across all frequencies $f \in \mathcal{F}$.

We can transform (5) into a consensus optimization problem as follows. First, we create the augmented Lagrangian as

$$L_f(\mathbf{J}_f, \mathbf{Z}, \mathbf{Y}_f) = g_f(\mathbf{J}_f) + \|\mathbf{Y}_f^H (\mathbf{J}_f - \mathbf{B}_f \mathbf{Z})\| + \frac{\rho_f}{2} \|\mathbf{J}_f - \mathbf{B}_f \mathbf{Z}\|^2 \quad (6)$$

where the subscript $(\cdot)_f$ denotes data (and parameters) at frequency f . In (6), $g_f(\mathbf{J}_f)$ is the original cost function as in (2). The Lagrange multiplier is given by $\mathbf{Y}_f \in \mathbb{C}^{2N \times 2}$. The global variable \mathbf{Z} is shared by data at all P frequencies. One noteworthy difference from our previous work [3], [22] is that rather than being fixed, the penalty parameter ρ_f is variable.

The ADMM iterations $n = 1, 2, \dots$ for solving (6) are given as

$$(\mathbf{J}_f)^{n+1} = \arg \min_{\mathbf{J}} L_f(\mathbf{J}, (\mathbf{Z})^n, (\mathbf{Y}_f)^n, \rho_f^n) \quad (7)$$

$$(\mathbf{Z})^{n+1} = \arg \min_{\mathbf{Z}} \sum_f L_f((\mathbf{J}_f)^{n+1}, \mathbf{Z}, (\mathbf{Y}_f)^n, \rho_f^n) \quad (8)$$

$$(\mathbf{Y}_f)^{n+1} = (\mathbf{Y}_f)^n + \rho_f^n ((\mathbf{J}_f)^{n+1} - \mathbf{B}_f (\mathbf{Z})^{n+1}) \quad (9)$$

$$\rho_f^{n+1} = \text{update penalty parameter} \quad (10)$$

where we use the superscript $(\cdot)^n$ to denote the n -th iteration where (7) to (10) are executed in order. The steps (7),(9) and (10) are done for each f in parallel, at each compute (slave) node. The slave nodes are distributed across a network of computers. The update of the global variable in (8) is done at the fusion center. The extra step (10), which is an improvement from our previous work [3], [22], will be discussed in section III.

III. UPDATING PENALTY PARAMETER

Since the constraint $\mathbf{J}_f = \mathbf{B}_f \mathbf{Z}$ in (5) is not guaranteed to be entirely accurate, increasing the value of ρ_f too much would bias the solutions towards this constraint and therefore increase the estimation error. Moreover, the observed data \mathbf{V}_{pqf} in (1) always contain contributions from weak signals from the sky that are not part of the sky model \mathbf{C}_{pqf} [28], [29] and we do not expect to see continued improvement of solutions with increased number of ADMM iterations. Hence, in this paper, we use a fixed number of ADMM iterations rather than using various stopping criteria [2].

We compare two popular schemes for the update of the penalty parameter, which can be plugged in to (10) of the ADMM iterations. In both cases, the initial value ($n = 1$) for

ρ_f^1 is chosen by using the magnitude of the lowest eigenvalue of the Hessian, say $|\lambda|$, (scaled down by a factor $\approx 1/10$) as described in [22]. In addition, to safeguard that the updated ρ_f^n does not increase too much, thereby giving too much weight to the constraint in (6), $|\lambda|$ is also used as an upper bound to all updates of ρ_f . In other words, if a possible update of ρ_f is higher than $|\lambda|$, it is clamped at this value.

A. Residual balancing penalty update

The idea behind the residual balancing method [2], [17], [18] is to select penalty parameter such that both the primal residual \mathbf{R}_f^n

$$\mathbf{R}_f^n = \mathbf{J}_f^n - \mathbf{B}_f \mathbf{Z}^n \quad (11)$$

and the dual residual \mathbf{S}_f^n

$$\mathbf{S}_f^n = \rho_f^n \mathbf{B}_f (\mathbf{Z}^n - \mathbf{Z}^{n-1}) \quad (12)$$

have balanced norms. This provides a balance between the original cost function and the constraint in (6). Heuristically, the penalty parameter is updated as

$$\rho_f^{n+1} = \begin{cases} \tau \rho_f^n & \text{if } \|\mathbf{R}_f^n\| > \mu \|\mathbf{S}_f^n\| \\ \tau^{-1} \rho_f^n & \text{if } \|\mathbf{R}_f^n\| < \mu^{-1} \|\mathbf{S}_f^n\| \\ \rho_f^n & \text{otherwise,} \end{cases} \quad (13)$$

where $\mu (> 1)$ and $\tau (> 1)$ are two constants that are given a priori and typical values used are $\mu = 10$ and $\tau = 2$ [2].

B. Spectral penalty update

The spectral parameter update [19], [20] is based on the Barzilai-Borwein method [23] used in adaptive step size selection of gradient descent optimization schemes [30]. For this scheme, we need extra variables that have the lifetime of the total ADMM iterations, i.e., $\widehat{\mathbf{Y}}_f^0, \widehat{\mathbf{Y}}_f, \mathbf{J}_f^0 \in \mathbb{C}^{2N \times 2}$. At the first ADMM iteration ($n = 1$), using the current solutions $(\mathbf{J}_f)^1$, initialize $\widehat{\mathbf{Y}}_f^0 = \mathbf{J}_f^0 = (\mathbf{J}_f)^1$. It is also noteworthy that the penalty is not updated at each ADMM iteration, on the contrary, it is done with a periodicity $T (\geq 2)$. At the n -th ADMM iteration, if n is a multiple of T , we perform an update as follows. First, we find step sizes α_{SD}, α_{MG} (the subscripts SD and MG stand for steepest descent and minimum gradient [30]) and correlation coefficient α as

$$\left(\widehat{\mathbf{Y}}_f\right)^{n+1} = (\mathbf{Y}_f)^n + \rho_f^n ((\mathbf{J}_f)^{n+1} - \mathbf{B}_f (\mathbf{Z})^n), \quad (14)$$

$$\Delta \mathbf{Y}_f = \left(\widehat{\mathbf{Y}}_f\right)^{n+1} - \widehat{\mathbf{Y}}_f^0, \quad \Delta \mathbf{J}_f = (\mathbf{J}_f)^{n+1} - \mathbf{J}_f^0, \quad (15)$$

$$\delta_{11} = \text{trace}(\text{real}(\Delta \mathbf{Y}_f^H \Delta \mathbf{Y}_f)) \quad (16)$$

$$\delta_{12} = \text{trace}(\text{real}(\Delta \mathbf{Y}_f^H \Delta \mathbf{J}_f))$$

$$\delta_{22} = \text{trace}(\text{real}(\Delta \mathbf{J}_f^H \Delta \mathbf{J}_f)),$$

$$\alpha = \frac{\delta_{12}}{\sqrt{\delta_{11} \delta_{22}}}, \quad \alpha_{SD} = \frac{\delta_{11}}{\delta_{12}}, \quad \alpha_{MG} = \frac{\delta_{12}}{\delta_{22}}. \quad (17)$$

Note that (14) differs from (9) because $(\mathbf{Z})^n$ is used in the former and $(\mathbf{Z})^{n+1}$ is used in the latter. Next, a candidate for the updated penalty $\hat{\alpha}$ is chosen as

$$\hat{\alpha} = \begin{cases} \alpha_{MG} & \text{if } 2\alpha_{MG} > \alpha_{SD} \\ \alpha_{SD} - \frac{\alpha_{MG}}{2} & \text{otherwise.} \end{cases} \quad (18)$$

Finally, if there is sufficient correlation for this update,

$$\rho_f^{n+1} = \begin{cases} \hat{\alpha} & \text{if } \alpha \geq \underline{\alpha} \\ \rho_f^n & \text{otherwise} \end{cases} \quad (19)$$

where $\underline{\alpha}$ is a constant (typically > 0.2) to ensure the new update is not a spurious result. At the last step, the auxiliary variables are updated as

$$\widehat{\mathbf{Y}}_f^0 = \left(\widehat{\mathbf{Y}}_f\right)^{n+1}, \quad \mathbf{J}_f^0 = (\mathbf{J}_f)^{n+1} \quad (20)$$

to be used in the next update of the penalty.

We compare the performance of both aforementioned methods in section IV. Comparing the computational cost, the residual balancing method is simpler but the spectral method is also not expensive as all what is needed is a few linear operations and inner products. Moreover, the spectral update is not performed at every ADMM iteration.

IV. SIMULATION RESULTS

We simulate an array of $N = 47$ receivers that calibrate along $K = 4$ directions in the sky. The settings for the simulations are quite similar to the one used in [22]. The matrices corresponding to the systematic errors, i.e., $\mathbf{J}_{pk}, \mathbf{J}_{qk}$ in (1) are generated with their elements having values drawn from a complex uniform distribution in $[0, 1]$, multiplied by a frequency dependence given by a random 8-th order ordinary polynomial in frequency. The intensities of the $K = 4$ sources are randomly generated in the range $[1, 5]$ intensity units and their positions are randomly chosen in a field of view of about 7×7 square degrees. The variation of intensities with frequency is given by a power law with randomly generated exponent in $[-1, 1]$. The noise matrices \mathbf{N}_{pq} in (1) are simulated to have complex circular Gaussian random variables. The variance of the noise is changed according to the signal to noise ratio (SNR = 30)

$$\text{SNR} \triangleq \frac{\sum_{p,q} \|\mathbf{V}_{pq}\|^2}{\sum_{p,q} \|\mathbf{N}_{pq}\|^2}. \quad (21)$$

In addition, we add the signals of 400 weak sources, with intensities uniformly distributed in $[0.01, 0.1]$ intensity units, randomly located within the 7×7 square degrees field of view. The signals of these 400 weak sources act as an additional source of noise and are simulated without any systematic errors.

We generate data for $P = 8$ frequency channels in the range 115 to 185 MHz. For calibration, we setup a 3-rd order polynomial model ($F = 4$), using Bernstein basis functions [31] for the matrix \mathbf{B}_f in (6). We intentionally use a lower order frequency dependence than what is actually present in the data to create a realistic scenario where the exact model for the systematic errors is not known. Initial values for the calibration parameters are always set as $\mathbf{J}_p = \mathbf{I}$ for $p \in [1, N]$. The penalty parameter for the K directions are initialized using $1/10$ of the magnitude of the lowest eigenvalue of the Hessian of (2), as described in [22]. The magnitude of the lowest eigenvalue is also used as an upper bound to any updated value of the penalty.

The accuracy of calibration is measured using the normalized (and averaged over all directions) mean squared error

(NMSE) between true \mathbf{J}_f and its estimate as

$$\text{NMSE} \triangleq \frac{1}{\sqrt{2KN}} \sqrt{\sum_{\text{over all } k} \|\mathbf{J}_f - \hat{\mathbf{J}}_f \mathbf{U}\|^2} \quad (22)$$

where \mathbf{U} is a unitary matrix that removes the unitary ambiguity in the estimated $\hat{\mathbf{J}}_f$ [32].

We compare the spectral penalty update (with $T = 2$ and $\underline{\alpha} = 0.2$), and the residual balance penalty update (with $\mu = 20$ and $\tau = 2$) against the performance of ADMM with a fixed penalty. In Fig. 1, we show the variation of ρ_f with ADMM iterations for both adaptive schemes, for one direction (out of K) and frequency.

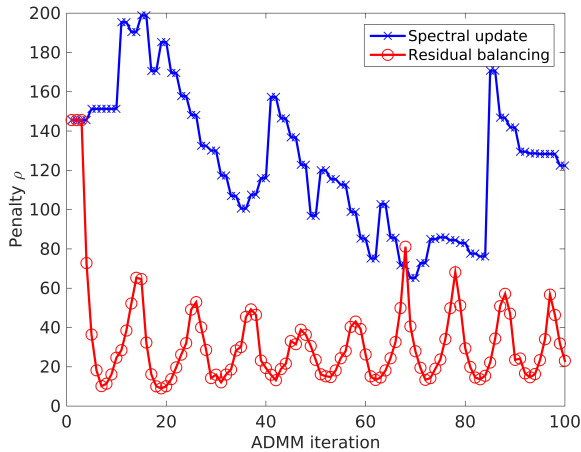


Fig. 1. Variation of ρ_f for the two adaptive update schemes with ADMM iteration.

In Fig. 2, we show the variation of NMSE (averaged over all frequencies) with ADMM iterations, for both adaptive penalty updated schemes as well as for the case where the penalty is fixed. In all cases, the initial penalty parameter is the same. We see that while both adaptive update schemes perform better than ADMM with a fixed penalty, the residual balance update scheme shows more oscillations.

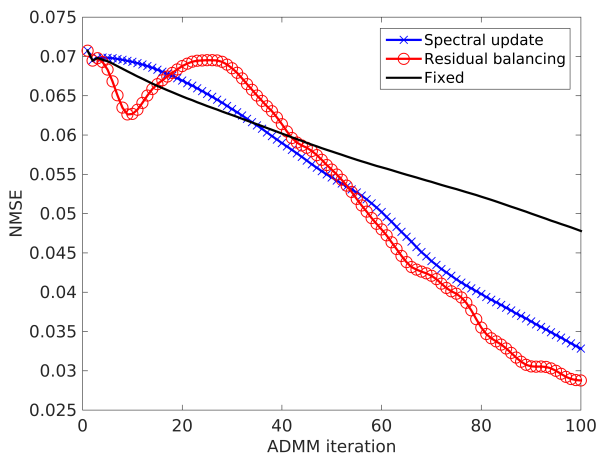


Fig. 2. NMSE (averaged over all frequencies) variation, with ADMM iteration.

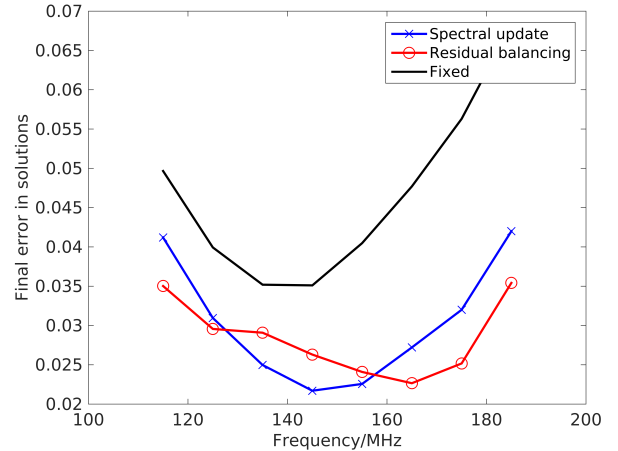


Fig. 3. Final NMSE after 100 ADMM iterations.

In Fig. 3, we show the final NMSE (after 100 ADMM iterations) for all $P = 8$ frequencies. Both adaptive penalty update methods have better NMSE than ADMM with a fixed penalty. In a real observation, data is calibrated by taking small segments and for a full observation, calibration such as the one simulated in this example has to be carried out thousands of times. Hence, rather than continuing ADMM iterations until convergence, the iterations are halted at a predefined value. Therefore, calibration schemes that show less oscillations in NMSE are better suited. Therefore, we give preference to the spectral penalty update as a practical calibration scheme.

V. CONCLUSIONS

We have compared the performance of adaptive penalty update in ADMM applied to distributed radio interferometric calibration. We used two popular penalty update schemes, namely the residual balancing update and the spectral (Barzilai-Borwein) update. Both methods improve performance of calibration compared with ADMM with a fixed penalty parameter. However, the spectral penalty update shows more stability and is preferable in practical applications. Software for distributed radio interferometric calibration with the spectral penalty parameter update is available at <http://sagecal.sf.net/> and <https://github.com/nlesc-dirac/sagecal>.

ACKNOWLEDGMENT

This work is supported by Netherlands eScience Center (project DIRAC, grant 27016G05) and the European Research Council (project LOFARCORE, grant 339743).

REFERENCES

- [1] D. Bertsekas and J.N. Tsitsiklis, *Parallel and Distributed Computation: Numerical Methods*, 2nd edition, Singapore: Athena Scientific, 1997.
- [2] Stephen Boyd, Neal Parikh, Eric Chu, Borja Peleato, and Jonathan Eckstein, "Distributed optimization and statistical learning via the alternating direction method of multipliers," *Foundations and Trends® in Machine Learning*, vol. 3, no. 1, pp. 1–122, 2011.
- [3] S. Yatawatta, "Distributed radio interferometric calibration," *MNRAS*, vol. 449, no. 4, pp. 4506–4514, 2015.

- [4] M. Brossard, M. N. El Korso, M. Pesavento, R. Boyer, P. Larzabal, and S. J. Wijnholds, "Parallel Calibration for Sensor Array Radio Interferometers," *ArXiv e-prints*, Sept. 2016.
- [5] C. Meillier, P. Bianchi, and W. Hachem, "Two distributed algorithms for the deconvolution of large radio-interferometric multispectral images," in *2016 24th European Signal Processing Conference (EUSIPCO)*, Aug 2016, pp. 728–732.
- [6] J. Deguignet, A. Ferrari, D. Mary, and C. Ferrari, "Distributed multi-frequency image reconstruction for radio-interferometry," in *2016 24th European Signal Processing Conference (EUSIPCO)*, Aug 2016, pp. 1483–1487.
- [7] A. Onose, R. E. Carrillo, J. D. McEwen, and Y. Wiaux, "A randomised primal-dual algorithm for distributed radio-interferometric imaging," in *2016 24th European Signal Processing Conference (EUSIPCO)*, Aug 2016, pp. 1448–1452.
- [8] A. Onose, A. Dabbech, and Y. Wiaux, "An accelerated splitting algorithm for radio-interferometric imaging: when natural and uniform weighting meet," *ArXiv e-prints*, Jan. 2017.
- [9] Yan Yang, Jian Sun, Huibin Li, and Zongben Xu, "ADMM-Net: A deep learning approach for compressive sensing MRI," *arXiv preprint arXiv:1705.06869*, 2017.
- [10] Simon Setzer, "Operator splittings, Bregman methods and frame shrinkage in image processing," *International Journal of Computer Vision*, vol. 92, no. 3, pp. 265–280, 2011.
- [11] Kuang Gong, Guobao Wang, Kevin T. Chen, Ciprian Catana, and Jinyi Qi, "Nonlinear PET parametric image reconstruction with MRI information using kernel method," in *Proc. SPIE*, 2017, vol. 10132, pp. 101321G–101321G–7.
- [12] P. Giselsson and S. Boyd, "Linear Convergence and Metric Selection for Douglas-Rachford Splitting and ADMM," *ArXiv e-prints*, Oct. 2014.
- [13] Robert Nishihara, Laurent Lessard, Benjamin Recht, Andrew Packard, and Michael I. Jordan, "A general analysis of the convergence of ADMM," in *International Conference on Machine Learning 32*, 2015.
- [14] A. Teixeira, E. Ghadimi, I. Shames, H. Sandberg, and M. Johansson, "The ADMM algorithm for distributed quadratic problems: Parameter selection and constraint preconditioning," *Signal Processing, IEEE Transactions on*, vol. 64, no. 2, pp. 290–305, Jan 2016.
- [15] E. Ghadimi, A. Teixeira, I. Shames, and M. Johansson, "Optimal parameter selection for the alternating direction method of multipliers (ADMM): Quadratic problems," *Automatic Control, IEEE Transactions on*, vol. 60, no. 3, pp. 644–658, March 2015.
- [16] Mingyi Hong, Zhi-Quan Luo, and M. Razaviyayn, "Convergence analysis of alternating direction method of multipliers for a family of nonconvex problems," in *Acoustics, Speech and Signal Processing (ICASSP), 2015 IEEE International Conference on*, April 2015, pp. 3836–3840.
- [17] B. S. He, H. Yang, and S. L. Wang, "Alternating direction method with self-adaptive penalty parameters for monotone variational inequalities," *Journal of Optimization Theory and Applications*, vol. 106, no. 2, pp. 337–356, 2000.
- [18] B. Wohlberg, "ADMM Penalty Parameter Selection by Residual Balancing," *ArXiv e-prints*, Apr. 2017.
- [19] Z. Xu, M. A. T. Figueiredo, and T. Goldstein, "Adaptive ADMM with Spectral Penalty Parameter Selection," *ArXiv e-prints*, May 2016.
- [20] Z. Xu, S. De, M. Figueiredo, C. Studer, and T. Goldstein, "An Empirical Study of ADMM for Nonconvex Problems," *ArXiv e-prints*, Dec. 2016.
- [21] Z. Xu, G. Taylor, H. Li, M. Figueiredo, X. Yuan, and T. Goldstein, "Adaptive Consensus ADMM for Distributed Optimization," *ArXiv e-prints*, June 2017.
- [22] S. Yatawatta, "Fine tuning consensus optimization for distributed radio interferometric calibration," in *2016 24th European Signal Processing Conference (EUSIPCO)*, Aug 2016, pp. 265–269.
- [23] J. Barzilai and J.M. Borwein, "Two-point step size gradient methods," *IMA Journal of Numerical Analysis*, vol. 8, no. 1, pp. 141, 1988.
- [24] J. P. Hamaker, J. D. Bregman, and R. J. Sault, "Understanding radio polarimetry, paper I," *Astronomy and Astrophysics Supp.*, vol. 117, no. 137, pp. 96–109, 1996.
- [25] A.R. Thompson, J.M. Moran, and G.W. Swenson, *Interferometry and synthesis in radio astronomy (3rd ed.)*, Wiley Interscience, New York, 2001.
- [26] J.A. Fessler and A.O. Hero, "Space alternating generalized expectation maximization algorithm," *IEEE Trans. on Sig. Proc.*, vol. 42, no. 10, pp. 2664–2677, Oct. 1994.
- [27] S. Kazemi, S. Yatawatta, S. Zaroubi, P. Labropoulos, A.G. de Bruyn, L. Koopmans, and J. Noordam, "Radio interferometric calibration using the SAGE algorithm," *MNRAS*, vol. 414, no. 2, pp. 1656–1666, June 2011.
- [28] S. Kazemi and S. Yatawatta, "Robust radio interferometric calibration using the t-distribution," *MNRAS*, vol. 435, pp. 597–605, Oct. 2013.
- [29] V. Ollier, M. N. El Korso, R. Boyer, P. Larzabal, and M. Pesavento, "Robust Calibration of Radio Interferometers in Non-Gaussian Environment," *ArXiv e-prints*, Dec. 2016.
- [30] Bin Zhou, Li Gao, and Yu-Hong Dai, "Gradient methods with adaptive step-sizes," *Comput. Optim. Appl.*, vol. 35, no. 1, pp. 69–86, Sept. 2006.
- [31] R. T. Farouki and V. T. Rajan, "Algorithms for polynomials in Bernstein form," *Comput. Aided Geom. Des.*, vol. 5, no. 1, pp. 1–26, June 1988.
- [32] S. Yatawatta, "On the interpolation of calibration solutions obtained in radio interferometry," *MNRAS*, vol. 428, no. 1, pp. 828–833, Jan. 2013.